

Extended depth-of-field and 3D information extraction in digital holographic microscopy

Isabelle Bergoënd¹, Tristan Colomb², Nicolas Pavillon¹, Yves Emery² and Christian Depeursinge¹

¹Laboratory of Applied Optics, Ecole Polytechnique Fédérale de Lausanne (EPFL), CH-1015 Lausanne, Switzerland

²Lycée Tec SA, PSE-A, CH-1015 Lausanne, Switzerland

Corresponding author: isabelle.bergoend@epfl.ch

Abstract: A comparison of algorithms for depth-of-field extension in the particular field of digital holographic microscopy is presented. Using the reconstruction properties of holography, a simple 3D reconstruction method from a single hologram is deduced.

©2009 Optical Society of America

OCIS codes: (090.1995) Digital holography; (100.6890) Three-dimensional image processing; (180.0180) Microscopy

1. Introduction

The limited depth-of-field is a main drawback of microscopy that prevents from observing, for example, thick semi-transparent objects with all their features focalized at the same time. Several algorithms have been developed during the past years to fusion images having various planes of focus and thus obtain a completely focalized image.

Nevertheless, in classic microscopy only a limited step that can be imposed on the mechanical system to change the focus plane. Digital holographic microscopy overcomes this disadvantage by permitting an image reconstruction in any plane parallel to the hologram plane. The reconstruction plane can therefore be moved with an arbitrary step. Moreover, digital holography gives access not only to the image intensity but also to the phase carrying information on the variations of refraction index, which may be very useful to observe internal structures into transparent biological objects.

Most of the extended depth-of-field algorithms used in classic microscopy aim at merging several images of the same object, each of them being partially focalized, depending on the distance of each inner object. To find the focalized regions, one of the first idea consisted in looking for the extrema of amplitude [1]. This method gives satisfying results only when the image has a good contrast everywhere. Better results are obtained when calculating the energy contained in each region of the high-pass filtered images [2]. Many methods, like gradient or Tenengrad's method, use the pixels in the neighbourhood of the current one and define a criterion of sharpness [1,3-6]. Another suggestion is the reconstruction of the focalized image using, for each pixel, a linear combination of the corresponding pixels taken from each of the partially focalized images [7]. Ferraro *et al.* studied the focalization and 3D reconstruction especially in holographic microscopy using the distance information carried by the phase image [8,9]. Wavelet methods, due to their ability to compute localized spatial frequencies, are sometimes used to reconstruct focalized images [10]. Fresnelets were especially developed for holographic purposes [11].

In this paper, we present a comparison of various existing algorithms for depth-of-field extension that we especially apply to digital holographic microscopy. Then, using the inherent ability of these algorithms to retain the distance of each in-focus region, we perform a 3D reconstruction of the objects of interest, using phase images.

2. Principle of computation of the focalized image

In digital holography, a stack of images, reconstructed at various distances, can easily be obtained from a single experimental hologram acquisition. It avoids any problem of misalignment or object modification from one image to the other, and it is also well suited to depth-of-field extension. In our case, from a hologram typically recorded in transmission through a microscope objective using a Mach-Zehnder interferometer, we select the virtual image in the Fourier plane and compute a numerical parametric lens in order to correct the tilt aberration, the phase offset and the wavefront curvature [12]. The mean focus distance, roughly corresponding to the centre of the thick specimen, is found visually or using an autofocus algorithm [13]. A range of distances to be investigated and a longitudinal step are then chosen to generate the stack of images. Two conditions are respected:

- the range of reconstruction distances covers the entire object thickness, thus every part is in focus in at least one image of the stack
- the step is less than the microscope depth-of-field so that the object thickness is over-sampled.

As any reconstruction distance can be computed in digital holography, these conditions can always be fulfilled.

From this stack of images, we compute several algorithms for depth-of-field extension and compare the final

focalized images. As our second purpose is to perform a 3D reconstruction, we mostly make use of algorithms that retain one slice of the stack (one distance of focus) for each pixel. The chosen methods are: (1) sum-modified Laplacian [4], (2) variance [5], (3) mean longitudinal value of intensity weighted with spatial variance, (4) Tenengrad [5], (5) Pieper and Korpel's differential operator [1], (6) gradient [3] and (7) Eltoukhy's linear combination [7]. We also use (8) the software developed by B. Forster et al. [10] to compare the previous algorithms with a wavelets-based method, here complex Daubechies wavelets. For every method using the pixel's neighbourhood (1-4 and 6-7), we compute the criterion pixel by pixel in a $N \times N$ region ($3 \leq N \leq 25$) and shift the region with overlapping to compute the next pixel. To save time, it is possible not to overlap the regions.

3. Results of the comparison of algorithms for depth-of-field extension in digital holographic microscopy

The main existing comparisons of extended depth-of-field algorithms use a set of images artificially generated from which one image is the reference focalized image and the others are partially blurred, so that an error between the reference image and the reconstructed one can be calculated. In the absence of such an image, which is our case because the biological objects we are using can only be observed with a microscope (thus with limited depth-of-field), it is not easy to find a criterion of measurement of the quality of the focalization. We choose two criteria. The first one involves the width measurement of some elements in their plane of focus, where they have the smallest size. This measurement is then compared with the corresponding one in the final image and a measurement error is calculated. The second criterion is a visual one, where we attribute a mark to the final images according to the visibility of the expected features located at different distances in a biological specimen, also taking into account the number of the slice in which each pixel was taken. The same study was performed for $N = 3$, $N = 15$ and $N = 25$ for the concerned algorithms. The results are presented in table 1.

Table 1: Best-marked algorithms for the size measurement, visual appreciation and execution time criteria. Last row: all the tested methods are taken into account. Other rows: only those using varying N are considered.

	Object measurement	Visual criterion	Execution time
Best algo. among 1-4 and 6-7, $N = 3$	Weighted mean (3)	Tenengrad (4)	Gradient (6)
Best algo. among 1-4 and 6-7, $N = 15$	Tenengrad (4)	Variance (2)	Gradient (6)
Best algo. among 1-4 and 6-7, $N = 25$	Variance (2)	Variance (2)	Gradient (6)
Best overall algorithm	Variance $N = 25$	Wavelets (8)	Pieper-Korpel (5)

A set of images, showing the resulting images of a selection of the tested algorithms, is given in fig. 2. As the object is a transparent amoeba, the phase images were used. Note that the result is no longer a quantitative phase map.

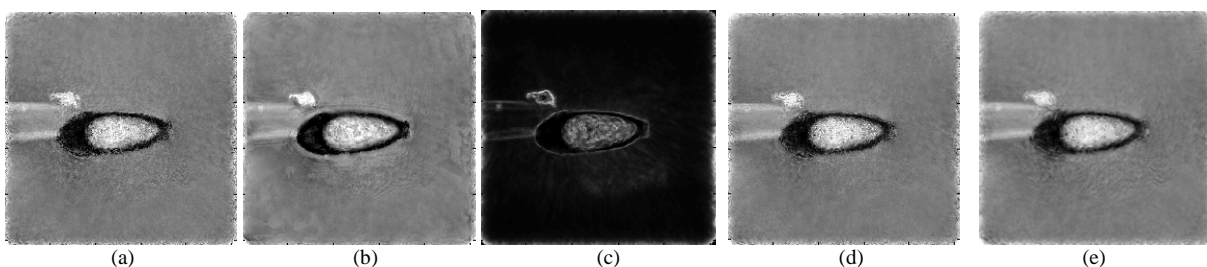


Fig. 1. Focalized phase images of an amoeba. a: Sum-modified Laplacian, $N = 3$. b: Variance, $N = 25$. c: Weighted mean, $N = 3$. d: Pieper-Korpel. e: Daubechies wavelets. B, c and e reproduce well the amoeba edges, but the internal structure is only partially visible in all images.

Let us make some remarks about the tested methods. The wavelet method and the variance method both give good visual results for the amoeba and both reach a measurement error less than 10%. We consider them as the best methods of depth-of-field extension for holographic microscopy, whereas variance execution time is among the longest ones. The variance method is suspected to reveal non-existing features when N is small, but this problem disappears for $N \geq 15$. The variance and the weighted mean well retrieve the object edges but perhaps not so well the internal structures having a weaker contrast. On the contrary, the sum-modified Laplacian does not reproduce precise edges, but works quite better for internal structures. The weighted mean acts more like a high-pass filter and does not preserve the image contrast (fig. 1. c), which may disturb the image understanding. Pieper and Korpel's

operator method is very fast and gives a visually satisfying focalized image, but with high-frequency noise in the map of the retrieved distances. Finally, Eltouky's method seems to be dependent on the order of the images in the stack and does not retrieve precisely the distances.

4. Extraction of 3D information

The algorithm chosen for this part of the study must give as an output a single value for the distance of focus for each pixel: the focalized image can not be composed of linear combinations of pixels of the stack or combinations of wavelets coefficients, because we are going to extract the 3D information from the distance of focus. We choose to use the variance criterion with $N = 15$, which is a good compromise between efficiency and computation time.

In a given focalized image, only a part of the image contains the object of interest, thus before performing the 3D reconstruction a selection of the region of interest has to be done. This is done by preserving only the pixels that exhibit a variance greater than a threshold. The threshold can be adjusted manually while the regions above the current threshold are automatically displayed. To avoid noise in the 3D reconstruction, the threshold must be very selective. After a spatial consistency check, dilatation and erosion are applied to close the contours. The groups of pixels included into a selected region are taken into the selection to ensure that the regions of interest are convex. Finally, the map composed of slices numbers computed by the variance algorithm is converted into a distance map calculated from the reconstruction distances of the stack. It is now possible to display a 3D view of the object.

Figure 2 shows the results obtained from the hologram of several small balls into a gel. The distances are well rendered, whereas some artefacts appear between the closest balls that are nearly in contact.

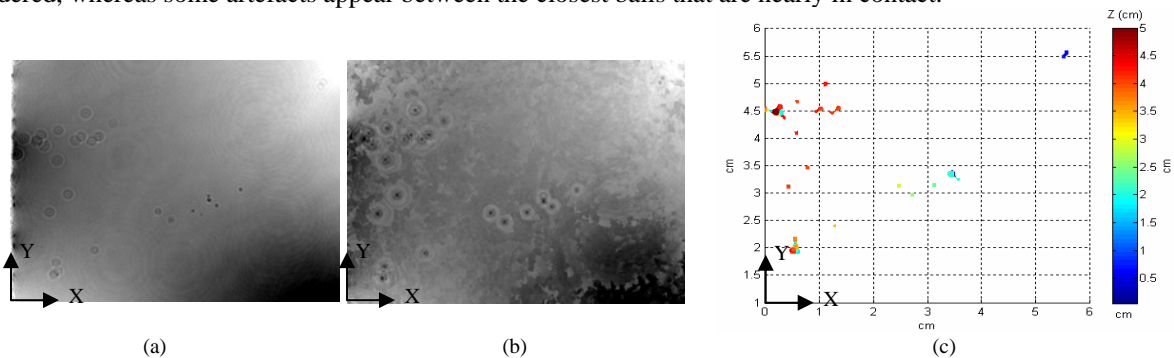


Fig. 2. a: One phase image from the stack, with balls in the centre in focus. b: Focalized phase image reconstructed using the variance method. c: Balls detected with their corresponding distance in the image plane.

This work is a part of the project “Real 3D” funded by the European Community's Seventh Framework.

5. References

- [1] R. J. Pieper, A. Korpel, “Image processing for extended depth of field”, *Appl. Optics*, **22**, 1449-1453 (1983).
- [2] H-S. Wu, J. Barba, J. Gil, “A focusing algorithm for high magnification cell imaging”, *Journal of Microscopy*, **184**, 133-142 (1996).
- [3] R.J. Wall, S.S. Sobin, M. Karspeck, R.G. Lindal, “Computer-derived image compositing”, *J. Appl. Physiol.*, **51**, 84-89 (1981).
- [4] S.K. Nayar and Y. Nakagawa, “Shape from focus”, *IEEE Trans. on Pattern Analysis and Machine Intelligence*, **16**, 824-831, (1994).
- [5] W. Huang and Z.L. Jing, “Evaluation of focus measures in multi-focus image fusion”, *Pattern Recognition Letters*, **28**, 493-500 (2007).
- [6] S.A. Sugimoto, “Digital composition of images with increased depth of focus considering depth information”, *Appl. Optics*, **24**, 2076 (1985).
- [7] H.A. Eltoukhy, S. Kavusi, “A Computationally Efficient Algorithm for Multi-Focus Image Reconstruction”, *Proc. of SPIE Electronic Imaging*, 332-341 (2003).
- [8] P. Ferraro, S. Grilli, D. Alfieri, S. De Nicola, A. Finizio, G. Pierattini, B. Javidi, G. Coppola, and V. Striano, “Extended focused image in microscopy by digital Holography”, *Optics Express*, **13**, 6738-6749 (2005).
- [9] G. Coppola, S. De Nicola, P. Ferraro, A. Finizio, S. Grilli, B. Javidi and G. Pierattini, “Holographic method with numerical reconstruction for obtaining an image of a three-dimensional object in which even points out of the depth of field are in focus, and holographic apparatus using such a method”, Patent number ITRM20050120 A1 (2006).
- [10] B. Forster, D. Van de Ville, J. Berent, D. Sage and M. Unser, “Complex wavelets for extended depth-of-field: a new method for the fusion of multichannel microscopy images”, *Microscopy Research and technique*, **65**, 33-42 (2004).
- [11] M. Liebling, Thierry Blu and M. Unser, “Fresnelets: new multiresolution wavelet bases for digital holography”, *IEEE Trans. On image processing*, **12**, 29-43 (2003).
- [12] T. Colomb, F. Montfort, J. Kühn, N. Aspert, E. Cuche, A. Marian, F. Charrière, S. Bourquin, P. Marquet and C. Depeursinge, “Numerical parametric lens for shifting, magnification and complete aberration compensation in digital holographic microscopy”, *J. Opt. Soc. Am. A*, **23**, 3177-3190 (2006).
- [13] P. Langehanenberg, B. Kemper, D. Dirksen and G. von Bally, “Autofocusing in digital holographic phase contrast microscopy on pure phase objects for live cell imaging”, *Appl. Optics*, **47**, 176-182 (2008).